Journal of Organometallic Chemistry 881 (2019) 45–50

Contents lists available at ScienceDirect

Journal of Organometallic Chemistry

journal homepage: www.elsevier.com/locate/jorganchem

Nickel(II) NHC-complexes with tridentate, dianionic ligands

Maximilian H. Clauberg [a], Darya Schmidt [a], Jörg Rust [b], Christian W. Lehmann [b], Natalia Arefyeva [c], Mathias Wickleder [c], Fabian Mohr [a, *]

[a] Fakultät für Mathematik und Naturwissenschaften, Anorganische Chemie, Bergische Universität Wuppertal, Gaußstr. 20, 42119, Wuppertal, Germany
[b] Chemische Kristallographie und Elektronenmikroskopie, Max-Planck-Institut für Kohlenforschung, Kaiser Wilhelm Platz 1, 45470, Mülheim an der Ruhr, Germany
[c] Department of Chemistry, Institute for Inorganic Chemistry, University of Cologne, Greinstr. 6, 50939, Cologne, Germany

ARTICLE INFO

Article history:
Received 28 September 2018
Received in revised form
26 November 2018
Accepted 29 November 2018
Available online 3 December 2018

Dedicated with best wishes to my mentor and friend Dick Puddephatt on the occasion of his 75th birthday.

Keywords:
Nickel
N-heterocyclic carbene
Sulfur-ligands
X-ray structure
Electrochemistry

ABSTRACT

A family of square planar nickel(II) complexes containing *N*-heterocyclic carbene ligands as well as tridentate, dianionic ligands was prepared by two different methods. The compounds were characterised by various spectroscopic methods and the solid-state structures were determined by single-crystal X-ray diffraction. Electrochemical studies of the compounds are also reported.

1. Introduction

N-heterocyclic carbenes (NHCs) once thought to be exotic and unstable chemical curiosities have evolved to a class of essential ligands with diverse and innovative applications in a variety of fields, especially homogenous catalysis and, more recently, in medicine [1–6]. Obvious reasons for the rapid growth of NHC-metal chemistry are their ease of preparation and handling and the fact that they form stable complexes with almost all known metals. Indeed, the discovery of the so-called "silver-oxide-route" by Lin and the use of the resulting silver(I) complexes to transfer the NHC ligand to other metals was a significant milestone in the development of NHC coordination chemistry [7]. Amongst the first transition metal NHC-complexes reported were nickel(II) species of the type $[Ni(X)_2(NHC)_2]$, formed by reaction of the free carbenes with suitable nickel precursors [8]. Since then, the diversity of nickel-NHC-complexes has steadily increased, mainly due to their superior performance in homogeneous catalysis. A number of recent reviews give an overview of preparation methods and applications of nickel NHC-complexes [9–11].

We have been interested in the medicinal properties of carbene or phosphine complexes the heavy group 10 metals Pd(II) and Pt(II) with sulfur-containing ligands [12–16]. Given the importance of nickel in biological systems, especially with sulfur-containing ligands [17–19], we report here results of our first experiments to prepare some nickel(II) NHC-complexes with sulfur-containing multidentate ligands.

2. Results and discussion

Our investigation began with the idea, that a cleavage reaction of sulfur-bridged dimeric nickel(II) compounds with *in situ* formed free carbenes should lead to the corresponding mononuclear Ni(II) NHC species. As a starting point for our investigation, we selected two different (known) sulfur-bridged dinickel(II) complexes, one with only sulfur donor atoms derived from 2-mercaptoethyl sulfide [20] and the other containing an S, N, O-donor set formed by condensation of 2-mercaptoaniline with acetylacetone [21]

* Corresponding author.
E-mail address: fmohr@uni-wuppertal.de (F. Mohr).

https://doi.org/10.1016/j.jorganchem.2018.11.034
0022-328X/

(denoted hereafter as $[Ni(L^{SSS})]_2$ and $[Ni(L^{SNO})]_2$, respectively). The reaction of these dinickel(II) species with two equivalents of the respective imidazolium salts in THF in the presence of a base (KO^tBu or NaHMDS) results in formation of brown solutions out of which dark orange solids can be isolated in low to moderate yields (Scheme 1).

The crude products contain paramagnetic impurities, as evidenced by broad lines in their proton NMR spectra. However, these can be removed by filtration through a short column of alumina. Pure, crystalline products were finally obtained after diffusing cyclohexane into THF solutions. As an alternative route, we envisaged the possibility, that silver(I) NHC-complexes could be used to transmetallate the carbene to the nickel centre. Indeed, to our delight the reaction of $[Ni(L^{SSS})]_2$ and $[Ni(L^{SNO})]_2$ with the silver(I) NHC complexes [IMesAgCl] [IMes = 1,3-dimesitylimidazolylidene] and [IPrAgCl] [IPr = 1,3-di(2,6-diisopropylphenyl)imidazolylidene] in a THF/CH_2Cl_2 mixture afforded orange-brown solutions accompanied by precipitation of AgCl (Scheme 2). The isolated orange-brown products were purified by the same procedures as detailed above (filtration through alumina and crystallisation from THF/cyclopentane). The purified products prepared by both methods are spectroscopically identical. Yields in both methods were similar, although consistently low in the case of the L^{SSS} ligand, due to losses during purification and crystallisation. We have however not optimised the purification methods to date. The nickel complexes appear to be stable to air and moisture both in solid-state and in solution.

The sharp lines and range of chemical shifts in the NMR spectra of the products are consistent with the presence of diamagnetic species. From the proton NMR spectra of the compounds a 1:1 ratio of tridentate ligand and NHC can be deduced. In the carbon NMR spectra of the products, the signal of the metal-bound carbon-atom has shifted from around 185 ppm in the silver(I) compounds [22] to 169 ppm (L^{SNO}) and 174 ppm (L^{SSS}) in the products. This is consistent with the formation of a nickel(II) NHC-complex. Similar chemical shifts for the carbenic carbon atom have been observed in the cyclopentadienyl nickel(II) NHC complex [CpNi(IMes)Cl] ($\delta_C = 168.0$) [23] and in bis(NHC) nickel(II) complexes of the type $[NiX_2(NHC)_2]$ ($\delta_C = 170.0$) [8,24]. The slight difference in this chemical shift is consistent for the presence of different donor atoms *trans* to carbon bound nickel atom in the two complexes. In the electrospray mass spectra of the compounds sodium adducts of the molecular ion peaks can be observed in addition to fragment peaks, which we were not able to assign. To confirm the proposed formulations, we obtained single crystals for X-ray diffraction experiments. The molecular structures are shown in Figs. 1 and 2 and important bond lengths and angles are collected in Table 1.

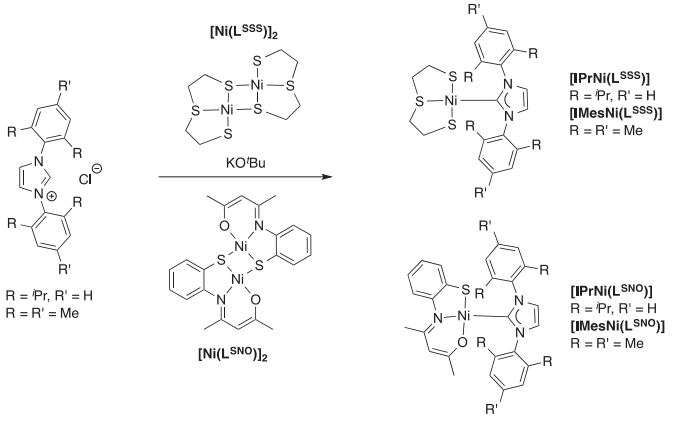

Scheme 1. Synthesis of the nickel(II) complexes via the free-carbene route.

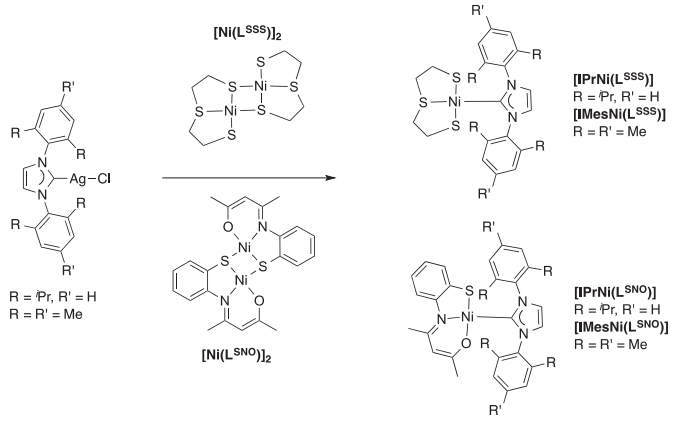

Scheme 2. Synthesis of the nickel(II) complexes via transmetallation.

Both compounds crystallise in the monoclinic crystal system in the space group $P2_1/n$. [IPrNi(L^{SSS})] (Fig. 1) consists of a nickel atom coordinated by the three sulfur atoms of the dianionic $[S,S,S]^{2-}$ ligand and the carbon atom of the NHC-ligand. Similarly, [IPrNi(L^{SNO})] (Fig. 2) contains a nickel atom coordinated by the sulfur, nitrogen and oxygen atoms of the dianionic $[S,N,O]^{2-}$ ligand and the carbon atom of the carbene. The coordination geometry about the metal centre is square planar for [IPrNi(L^{SNO})] and distorted square planar for [IPrNi(L^{SSS})], as determined using the τ_4-parameter proposed by Houser [25]. This value was calculated to be 0.05 for [IPrNi(L^{SNO})] and 0.26 for [IPrNi(L^{SSS})], clearly illustrating a greater distortion from square planar geometry ($\tau_4 = 0.00$ for perfect square planar coordination) of the latter compound. Inspection of the structures shows that the tridentate sulfur ligand seems responsible for this distortion. The two five-membered rings formed by the tri-sulfur ligand are evidently more rigid than the five- and six-membered chelate rings in [IPrNi(L^{SNO})]. The nickel-carbon bond lengths of 1.89 Å are similar to those observed in other Ni(II)–NHC-complexes including $[IPrNiCl_2(2,6\text{-lut})]$ [26] and $[IPrNi\{CH_2CHCHN(CH_2)_2NMe_2\}]$, containing a dianionic, tridentate $[C,N,N]^{2-}$ ligand [27]. In contrast to what is observed in the parent dimer $[Ni(L^{SSS})]_2$, where the three Ni–S bond lengths are 2.152(5),

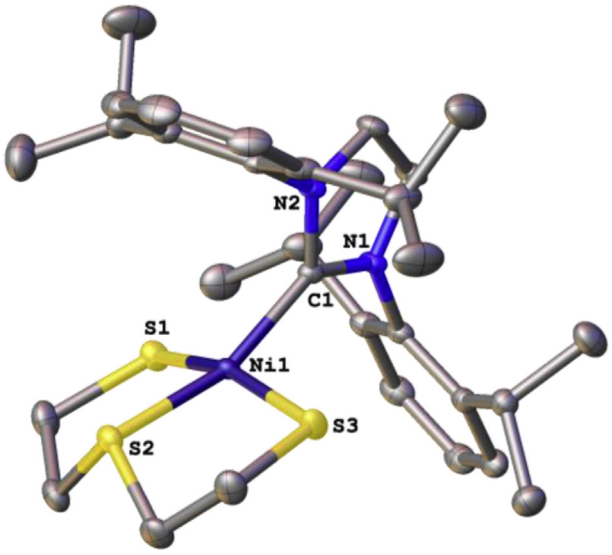

Fig. 1. Molecular structure of [IPrNi(L^{SSS})]. Ellipsoids are drawn at the 50% level. Hydrogen atoms have been omitted for clarity.

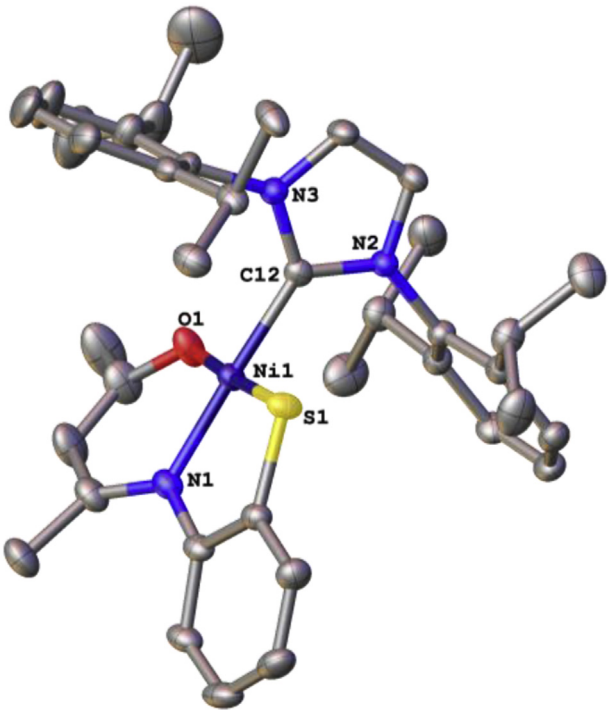

Fig. 2. Molecular structure of [IPrNi(L^{SNO})]. Ellipsoids are drawn at the 50% level. Hydrogen atoms have been omitted for clarity.

2.164(5) and 2.220(5) Å [28], the Ni-S_{trans} distance is shorter in the NHC complex than the two Ni-S_{cis} distances. Compared to the parent dimer [29], the Ni–N, Ni–O and Ni–S bond distances in [IPrNi(L^{SNO})] do not change significantly. In both compounds the carbene ligand lies perpendicular to the plane of the tridentate ligand, probably to minimise steric interactions.

2.1. Electrochemistry

Cyclic voltammograms of representative complexes (Figs. 3–5) were recorded in MeCN solutions at a scan speed of 100 mV s^{-1}. Selected electrochemical data is collected in Table 2.

For compounds [IPrNi(L^{SNO})] and [IMesNi(L^{SNO})] which contain the $[S,N,O]^{2-}$ ligand, irreversible waves are observed at 0.27 V and 0.28 V in the oxidation region, which originate from thiolate centred oxidation. In both compounds additional, irreversible oxidation peaks with potentials of 1.38 V and 0.75 V were present. These might result from further ligand-centred oxidation or its decomposition or arise from the Ni(II)/Ni(III) redox couple. In Cp-Ni(II) complexes containing NHC ligands values for the nickel oxidation in the range of 0.01–0.07 V have been reported [30].

Table 1
Selected bond distances and angles in [IPrNi(L^{SSS})] and [IPrNi(L^{SNO})].

Bond distances [Å]	[IPrNi(L^{SSS})]	[IPrNi(L^{SNO})]
Ni–C	1.8920(8)	1.890(2)
Ni–S	2.1757(3) Ni-S_{cis} 2.1856(3) Ni-S_{cis} 2.1400(3) Ni-S_{trans}	2.1293(7)
Ni–N	–	1.899(2)
Ni–O	–	1.8680(19)
Bond angles [°]		
C–Ni–N/S_{trans}	161.31(3)	175.55(9)
C–Ni–S_{cis}	90.71(3)	87.02(7)
C–Ni–O/S_{cis}	96.14(3)	90.00(9)
O/S_{cis}–Ni–S_{cis}	161.628(11)	176.96(6)

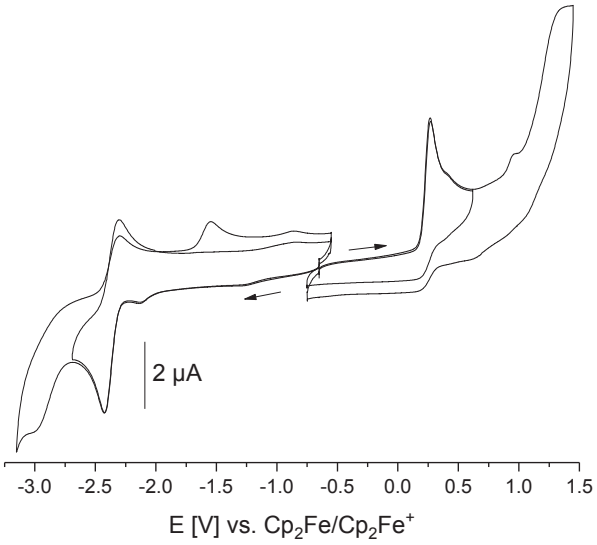

Fig. 3. Cyclic voltammograms of [IMesNi(L^{SNO})] in MeCN referenced to Cp_2Fe/Cp_2Fc^+.

In the cathodic region waves with peak potentials of −2.43 V and −2.48 V are observed. For [IMesNi(L^{SNO})] the wave shows partially reversible character, while for [IPrNi(L^{SNO})] the process appears irreversible. These reduction processes correspond to the Ni(II)/Ni(I) redox couple. The assignments are supported by DFT calculations of the complexes. The greatest contribution to the HOMO originates from the sulfur atoms and the aromatic ring, in case of the $[S,N,O]^{2-}$ ligand, with little involvement of the nickel (Fig. 6). The LUMO on the other hand, shows a contribution of the Ni d_{x2-y2} orbital, consistent with metal centred first reduction.

The compound containing the $[S,S,S]^{2-}$ ligand shows slightly more complex electrochemical behaviour. Here, the irreversible oxidation wave assigned to a mixed S/Ni-centred oxidation is at −0.07 V, with an additional, probably ligand-related, oxidation peak at 1.07 V. For reduction, one pseudo-reversible process at −2.44 V (nickel reduction) and one irreversible process

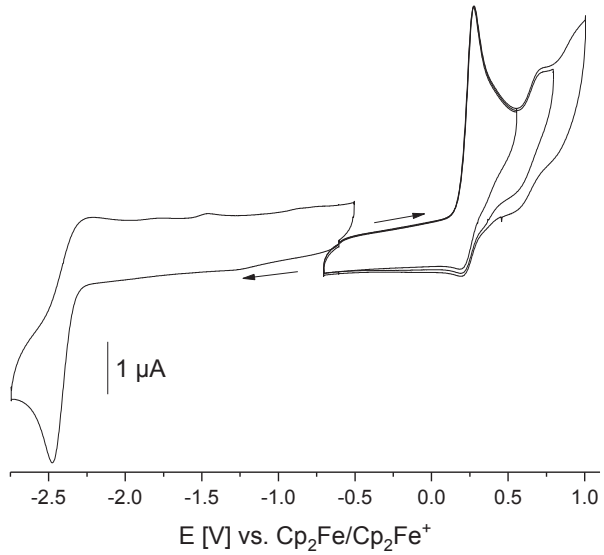

Fig. 4. Cyclic voltammograms of [IPrNi(L^{SNO})] in MeCN referenced to Cp_2Fe/Cp_2Fc^+.

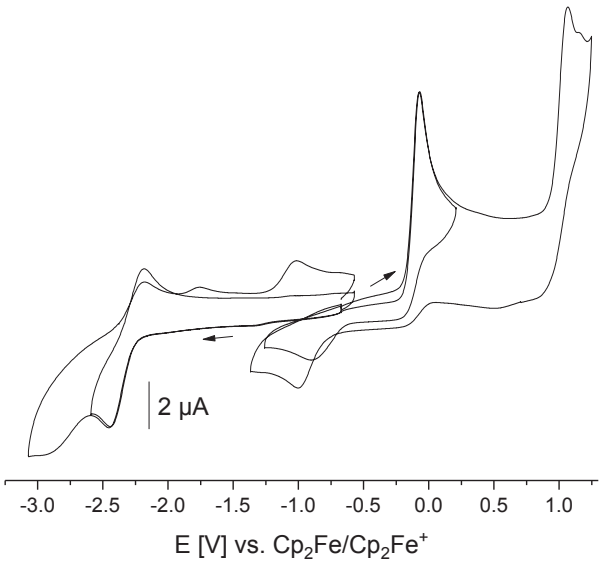

Fig. 5. Cyclic voltammograms of [IPrNi(L^{SSS})] in MeCN referenced to Cp_2Fe/Cp_2Fc^+.

Table 2
Selected electrochemical data.[1]

	Ox3	Ox2	Ox1	Red1	Red2
[IMesNi(L^{SNO})]		1.38 E_{pa}	0.27 E_{pa}	−2.43 E_{pc}	−3.03 E_{pc}
[IPrNi(L^{SNO})]	0.99 E_{pa}	0.75 E_{pa}	0.28 E_{pa}	−2.57 E_{pc}	
[IPrNi(L^{SSS})]		1.07 E_{pa}	−0.07 E_{pa}	−2.44 E_{pc}	−2.98 E_{pc}

[1] From cyclic voltammetry in 0.1 M nBu_4NPF_6/MeCN solutions at 100 mVs^{-1} scan rate. Potentials given in V *vs.* Cp_2Fe/Cp_2Fc^+. Anodic (E_{pa}) or cathodic (E_{pc}) peak potentials for irreversible processes.

at −2.98 V (ligand reduction) can be seen. In the parent dimer, an irreversible reduction wave was observed at −1.78 V for the nickel centre [31]. This is completely in line with the energy of the antibonding orbitals in octahedral and square planar d^8 systems.

In summary, we have prepared and characterized some nickel(II) NHC-complexes containing different tridentate co-ligands by two different methods. We are currently exploring the generality and scope of this class of compounds as well as some applications including catalysis and electrocatalysis.

3. Experimental

3.1. General

Reactions were carried out under dinitrogen gas using HPLC grade solvents, which were stored over 3 Å molecular sieves. The dimeric nickel complexes $[Ni(L^{SSS})]_2$ [20] and $[Ni(L^{SNO})]_2$ [21], the imidazolium salts [IMes]HCl and [IPr]HCl [32] as well as the silver(I)−NHC complexes [IMesAgCl] and [IPrAgCl] [22,33] were prepared by published methods. All other chemicals were purchased from commercial suppliers and were used as received. NMR spectra were recorded on Bruker Avance 400 or Bruker Avance III 600 instruments. Signals were referenced externally to TMS (^1H and ^{13}C). Elemental analyses were obtained in-house using an Elementar Vario EL analyser. Electrospray mass spectra were recorded in positive ion mode on a Bruker Daltonics microTOF system using MeCN solutions of the compounds.

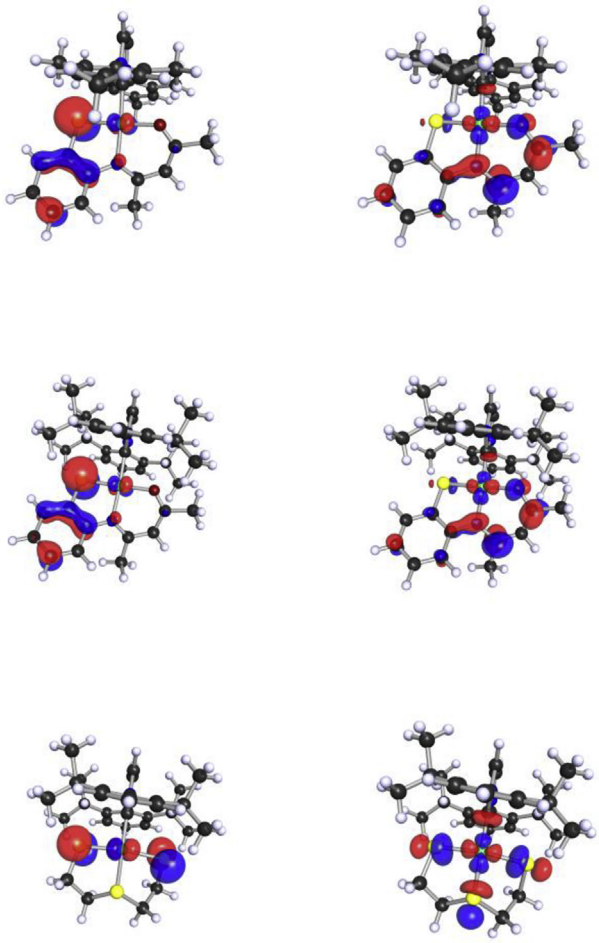

Fig. 6. HOMO (left) and LUMO (right) diagrams of [IMesNi(L^{SNO})] (top), [IPrNi(L^{SNO})] (middle) and [IPrNi(L^{SSS})] (bottom) from DFT calculations.

3.2. Synthesis of the Ni−NHC complexes

3.2.1. Method A. Free NHC method

To a solution of the dimeric Ni(II)-complex in THF (20 mL) was added the respective imidazolium chloride (2 equiv.) and KO^{t}Bu (2.3 equiv.) or NaHMDS (2.3 equiv.). The reaction mixture was heated to 60 °C for 2 h and then left at room temperature overnight. The solvent was removed under reduced pressure and the residue was extracted into CH_2Cl_2. This CH_2Cl_2 solution was passed through a short column of alumina. The eluting orange-brown solution was subsequently evaporated to dryness. Diffusion of cyclohexane into a THF solution afforded orange-brown crystals after several days. Samples for elemental analysis were further recrystallised from MeOH.

3.2.2. Method B. Ag-transmetallation method

To a solution of the dimeric Ni(II)-complex in a 1:1 THF/CH_2Cl_2 mixture (15 mL) was added the respective silver(I)−NHC complex (2 equiv.). After stirring the mixture at room temperature overnight, the solvent was removed in vacuum and the residue was extracted into CH_2Cl_2. This CH_2Cl_2 solution was passed through a short column of alumina. The eluting orange-brown solution was subsequently evaporated to dryness. Diffusion of cyclohexane into a THF solution afforded orange-brown crystals after several days.

3.2.3. [IMesNi(L^{SSS})]

This was prepared by method B as described above using

$[Ni(L^{SSS})]_2$ (0.100 g, 0.24 mmol) and [IMesAgCl] (0.203 g, 0.48 mmol). The product was obtained as an orange-brown solid in 27% yield. Using method A, the same product was obtained in 21% yield. ^{1}H NMR ($CDCl_3$): δ = 2.28–2.45 (m, 22 H, SCH_2CH_2S & Me), 2.62 (d, J = 10.8 Hz, 2 H, SCH_2CH_2S), 2.94 (d, J = 8.1 Hz, 2 H, SCH_2CH_2S), 6.92 (br. s, 1 H, imidazole-H), 7.07 (m, 5 H, imidazole-H & IMes). $^{13}C\{^1H\}$-NMR ($CDCl_3$): δ = 19.15 (Me), 19.34 (Me), 21.21 (Me), 30.46 (SCH_2CH_2S), 42.31 (SCH_2CH_2S), 124.28 (imidazole-C), 128.96 (IMes), 136.25 (IMes), 138.49 (IMes), 174.37 (CNi). Elemental analysis calcd. for $C_{25}H_{32}N_2S_3Ni$ MeOH (547.5): C 57.04, H 6.63, N 5.12; found: C 56.59, H 6.33, N 4.84%. ES-MS: m/z = 503 $[M+Na]^+$.

3.2.4. [IPrNi(L^{SSS})]

This was prepared by method B as described above using $[Ni(L^{SSS})]_2$ (0.050 g, 0.12 mmol) and [IPrAgCl] (0.109 g, 0.24 mmol). The product was obtained as an orange-brown solid in 26% yield. Using method A, the same compound was obtained in 32% yield. ^{1}H NMR ($CDCl_3$): δ = 1.07 (d, J = 7.7 Hz, 12 H, Me), 1.47 (d, J = 6.2 Hz, 12 H, Me), 2.18–2.32 (m, 4 H, SCH_2CH_2S), 2.53 (d, J = 8.1 Hz, 2 H, SCH_2CH_2S), 2.90 (d, J = 7.0 Hz, 2 H, SCH_2CH_2S), 3.14 (m, 4 H, CH), 7.02 (s, 2 H, imidazole-H), 7.33 (d, J = 7.4 Hz, 4 H, IPr), 7.48 (t, J = 7.4 Hz, 2 H, IPr). $^{13}C\{^1H\}$-NMR ($CDCl_3$): δ = 23.29 (Me), 26.21 (Me), 28.84 (CH), 30.58 (SCH_2CH_2S), 42.79 (SCH_2CH_2S), 123.68 (IPr), 125.16 (imidazole-C), 129.62 (IPr), 136.36 (IPr), 146.71 (IPr), C–Ni was not observed. Elemental analysis calcd. for $C_{31}H_{44}N_2S_3Ni$ MeOH (631.6): C 60.85, H 7.66, N 4.44; found: C 59.94, H 7.13, N 4.33%. ES-MS: m/z = 621 $[M+Na]^+$. X-ray quality crystals were obtained by vapour diffusion of cyclohexane into a THF solution of the complex.

3.2.5. [IMesNi(L^{SNO})]

This was prepared by method B as described above using $[Ni(L^{SNO})]_2$ (0.100 g, 0.19 mmol) and [IMesAgCl] (0.162 g, 0.38 mmol). The product was obtained as an orange-brown solid in 79% yield. Using method A, the same compound was obtained in 66% yield. ^{1}H NMR ($CDCl_3$): δ = 1.76 (s, 3 H, Me), 2.08 (s, 3 H, Me), 2.23 (s, 6 H, Me IMes), 2.36 (s, 12 H, Me IMes), 5.00 (s, 1 H, CH), 6.53 (dt, J = 7.4, 1.3 Hz, 1 H, Ar), 6.60 (t, J = 7.3 Hz, 1 H, Ar), 6.64 (d, J = 8.2 Hz, 1 H, Ar), 6.93 (s, 2 H, imidazole-H), 7.02 (s, 5 H, imidazole-H), 7.18 (dd, J = 7.0, 1.3 Hz, 1 H, Ar). $^{13}C\{^1H\}$-NMR ($CDCl_3$): δ = 18.08 (Me IMes), 19.12 (Me IMes), 21.19 (Me IMes), 24.06 (Me), 24.91 (Me), 102.97 (CH), 118.33 (Ar), 121.84 (Ar), 122.03 (Ar), 123.57 (imidazole-C), 126.92 (Ar), 128.99 (*m*-C Mes), 129.55 (*m*-C Mes), 136.00 (*ipso*-C Mes), 138.66 (*p*-C Mes), 143.89 (Ar), 147.65 (*o*-C Mes), 150.49 (CS), 163.48 (CN), 167.91 (CNi), 174.98 (CO). Elemental analysis calcd. for $C_{32}H_{35}N_2OSNi$ (568.4): C 67.62, H 6.21, N 7.39; found: C 67.63, H 6.17, N 7.42%. ES-MS: m/z = 590 $[M+Na]^+$.

3.2.6. [IPrNi(L^{SNO})]

This was prepared by method B as described above using $[Ni(L^{SNO})]_2$ (0.100 g, 0.19 mmol) and [IPrAgCl] (0.173 g, 0.38 mmol). The product was obtained as an orange-brown solid in 28%. Using method A, the same compound was obtained in 68% yield. ^{1}H NMR ($CDCl_3$): δ = 1.09 (d, J = 6.9 Hz, 12 H, IPr), 1.37 (d, J = 6.6 Hz, 12 H, IPr), 1.80 (s, 3 H, Me), 2.01 (s, 1 H, Me), 3.06 (m, 4 H, IPr), 4.96 (s, 1 H, CH), 6.48 (dt, J = 7.7, 1.5 Hz, 1 H, Ar), 6.54 (dt, J = 7.6, 1.3 Hz, 1 H, Ar), 6.58 (dd, J = 7.9, 1.0 Hz, 1 H, Ar), 6.99 (s, 2 H, imidazole-H), 7.07 (dd, J = 7.7, 1.5 Hz, 1 H, Ar), 7.34 (d, J = 7.7 Hz, 4 H, IPr), 7.47 (t, J = 7.7 Hz, 2 H, IPr). $^{13}C\{^1H\}$-NMR ($CDCl_3$): δ = 23.14 (IPr), 24.58 (Me), 25.71 (Me), 26.20 (IPr), 28.61 (IPr), 102.84 (CH), 118.21 (Ar), 121.68 (Ar), 121.83 (Ar), 124.05 (*m*-C IPr), 124.82 (imidazole-C), 126.55 (Ar), 129.96 (*p*-C IPr), 136.08 (*ipso*-C IPr), 144.37 (Ar), 146.52 (*o*-C IPr), 150.82 (CS), 163.12 (CN), 169.97 (CNi), 175.44 (CO). Elemental analysis calcd. for $C_{38}H_{47}NOSNi$ MeOH (684.6): C 68.42, H 7.51, N 6.14; found: C 68.86, H 7.31, N 6.22%. ES-MS: m/z = 674 $[M+Na]^+$. X-ray quality crystals were obtained by vapour diffusion of cyclohexane into a THF solution of the complex.

3.3. X-ray crystallography

Diffraction data were collected at 100 K using an Enraf-Nonius KappaCCD system located in front of a FR591 rotating anode equipped with an Incoatec focusing Montel optic for Mo radiation. For data integration the EVAL-14 package [34] was employed. For data scaling and absorption correction (combination of gaussian and multiscan corrections) SADABS was used. All crystal structures were solved using SHELXT and refined using SHELXL [35]. The Olex2 graphical user interface [36] was used for all structure manipulations and for molecular graphics. Crystallographic and refinement details are collected in Table 3.

Table 3
Crystallographic and refinement details for [IPrNi(L^{SSS})] and [IPrNi(L^{SNO})].

	[IPrNi(L^{SSS})]	[IPrNi(L^{SNO})]
CCDC code	1865725	1865724
Empirical formula	$C_{31}H_{44}N_2S_3Ni$	$C_{38}H_{47}N_3OSNi$
Formula weight	599.57	652.55
Crystal system	Monoclinic	Monoclinic
Space group	$P2_1/n$	$P2_1/n$
a/Å	10.1786(9)	11.0575(11)
b/Å	14.3692(13)	16.0914(16)
c/Å	22.224(2)	20.449(2)
β/°	99.143(2)	103.924(8)
Volume/Å^3	3209.1(5)	3531.6(6)
Z	4	4
ρ_{calc} g/cm^3	1.241	1.227
μ/mm^{-1}	0.821	0.641
F(000)	1280	1392
Crystal size/mm^3	0.06 × 0.143 × 0.200	0.04 × 0.13 × 0.24
θ range for data collection	2.336–33.320°	2.682–33.072°
Reflections collected	71470	40789
Independent reflections	12387 [R_{int} = 0.0273]	13338 [R_{int} = 0.0690]
Data/restraints/parameters	12387/0/342	13338/0/407
Goodness-of-fit on F^2	1.039	1.093
Final R indices [$I > 2\sigma(I)$]	R_1 = 0.0258 wR_2 = 0.0673	R_1 = 0.0674 wR_2 = 0.1577
R indices (all data)	R_1 = 0.0322 wR_2 = 0.0705	R_1 = 0.1199 wR_2 = 0.1859
Largest diff. peak and hole/eÅ^{-3}	0.6/-0.2	1.2/-1.1

3.4. Electrochemistry

Electrochemical measurements of the compounds were performed using a BioLogic Science Instruments model SP150 potentiostat controlled through the EC-Lab software interface. Experiments were performed in an electrochemical glass cell with a cell volume of 10 mL using 0.1 M $^{n}Bu_4NPF_6$ solutions in MeCN with a three-electrode configuration (glassy carbon working electrode, Pt counter electrode, Ag/AgCl pseudo reference electrode). The ferrocene/ferrocenium couple (Cp_2Fe/Cp_2Fe^{+}) served as internal reference.

3.5. DFT calculations

Calculations were performed using the TUBROMOLE program package [37] and TMoleX 4.2 [38] user interface. Structures were first geometry optimized at the def-SV(P)/B3LYP level [39–42] and were further optimized with the def2-TZVP basis set [43] for all atoms.

Appendix A. Supplementary data

Supplementary data to this article can be found online at https://doi.org/10.1016/j.jorganchem.2018.11.034.

References

[1] S.P. Nolan (Ed.), N-heterocyclic Carbenes in Synthesis, Wiley-VCH, Weinheim, 2006.
[2] F.E. Hahn, M.C. Jahnke, Angew Chem. Int. Ed. Engl. 47 (2008) 3122–3172.
[3] K.M. Hindi, M.J. Panzner, C.A. Tessier, C.L. Cannon, W.J. Youngs, Coord. Chem. Rev. 109 (2009) 3859–3884.
[4] S. Díez-González (Ed.), N-heterocylic Carbenes. From Laboratory Curiosities to Efficient Synthetic Tools, RSC Publishing, Cambridge, 2011.
[5] C. Hu, X. Li, W. Wang, R. Zhang, L. Deng, Curr. Med. Chem. 21 (2014) 1220–1230.
[6] S.P. Nolan (Ed.), N-heterocyclic Carbenes. Effective Tools for Organometallic Synthesis, Wiley-VCH, Weinheim, 2014.
[7] H.M.J. Wang, I.J.B. Lin, Organometallics 17 (1998) 972–975.
[8] W.A. Herrmann, G. Gerstberger, M. Spiegler, Organometallics 16 (1997) 2209–2212.
[9] A.P. Prakasham, P. Ghosh, Inorg. Chim. Acta. 431 (2015) 61–100.
[10] V. Ritleng, M. Henrion, M.J. Chetcuti, ACS Catal. 6 (2016) 890–906.
[11] Z.N. Gafurov, A.O. Kantyukov, A.A. Kagliev, A.A. Balabayev, O.G. Sinyashin, D.G. Yakhvarov, Russ. Chem. Bull. 66 (2017) 1529–1535.
[12] A. Molter, S. Kathrein, B. Kircher, F. Mohr, Dalton Trans. 47 (2018) 5055–5064.
[13] R. Rubbiani, E. Schuh, A. Meyer, J. Lemke, J. Wimberg, N. Metzler-Nolte, F. Meyer, F. Mohr, I. Ott, MedChemComm 4 (2013) 942–948.
[14] E. Guerrero, S. Miranda, S. Lüttenberg, N. Fröhlich, J.M. Koenen, F. Mohr, E. Cerrada, M. Laguna, A. Mendia, Inorg. Chem. 52 (2013) 6635–6647.
[15] P. Bippus, M. Skocic, M.A. Jakupec, B.K. Keppler, F. Mohr, J. Inorg. Biochem. 105 (2011) 462–466.
[16] S. Miranda, E. Vergara, F. Mohr, D. de Vos, E. Cerrada, A. Mendía, M. Laguna, Inorg. Chem. 47 (2008) 5641–5648.
[17] E. Bouwman, J. Reedijk, Coord. Chem. Rev. 249 (2005) 1555–1581.
[18] A. Sigel, H. Sigel, R.K.O. Sigel (Eds.), Nickel and its Surprising Impact in Nature, John Wiley & Sons, Chichester, 2007.
[19] S. Groysman, R.H. Holm, Biochemistry 48 (2009) 2310–2320.
[20] J. Harley-Mason, J. Chem. Soc. (1952) 146–149.
[21] G.R. Brubaker, J.C. Latta, D.C. Aquino, Inorg. Chem. 9 (1970) 2608–2610.
[22] P. de Frémont, N.M. Scott, E.D. Stevens, T. Ramnial, O.C. Lightbody, C.L.B. Macdonald, J.A.C. Clyburne, C.D. Abernethy, S.P. Nolan, Organometallics 24 (2005) 6301–6309.
[23] D.A. Malyshev, N.M. Scott, N. Marion, E.D. Stevens, V.P. Ananikov, I.P. Beletskaya, S.P. Nolan, Organometallics 25 (2006) 4462–4470.
[24] J. Berding, J.A. van Paridon, V.H.S. van Rixel, E. Bouwman, Eur. J. Inorg. Chem. (2011) 2450–2458.
[25] L. Yang, D.R. Powell, R.P. Houser, Dalton Trans. (2007) 955–964.
[26] C.H. Lee, D.A. Lutterman, D.G. Nocera, Dalton Trans. 42 (2013) 2355–2357.
[27] T. Takashi, O. Masato, O. Sensuke, Chem. Lett. 40 (2011) 248–249.
[28] G.A. Barclay, E.M. McPartlin, N.C. Atephenson, Acta Crystallogr. B25 (1969) 1262–1273.
[29] N. Ancin, S. Ide, S.G. Öztaş, M. Tüzün, J. Mol. Struct. 606 (2002) 45–50.
[30] F.P. Malan, E. Singleton, J. Conradie, M. Landman, J. Electroanal. Chem. 814 (2018) 66–76.
[31] H.J. Krüger, R.H. Holm, Inorg. Chem. 28 (1989) 1148–1155.
[32] L. Hintermann, Beilstein J. Org. Chem. 3 (2007) 1–5.
[33] R. Visbal, A. Laguna, M. Concepcion Gimeno, Chem. Commun. 49 (2013) 5642–5644.
[34] A.J.M. Duisenberg, L.M.J. Kroon-Batenburg, A.M.M. Schreurs, J. Appl. Crystallogr. 36 (2003) 220–229.
[35] G.M. Sheldrick, Acta Crystallogr. C71 (2015) 3–8.
[36] O.V. Dolomanov, L.J. Bourhis, R.J. Gildea, J.A.K. Howard, H. Puschmann, J. Appl. Crystallogr. 42 (2009) 339–341.
[37] Turbomole 7.0, a development of University of Karlsruhe and Forschungszentrum Karlsruhe GmbH, 2015.
[38] C. Steffen, K. Thomas, U. Huniar, A. Hellweg, O. Rubner, A. Schroer, J. Comput. Chem. 31 (2010) 2967–2970.
[39] A. Schafer, H. Horn, R. Ahlrichs, J. Chem. Phys. 97 (1992) 2571–2577.
[40] C.T. Lee, W.T. Yang, R.G. Parr, Phys. Rev. B, PRB 37 (1988) 785–789.
[41] A.D. Becke, J. Chem. Phys. 98 (1993) 5648–5652.
[42] A.D. Becke, J. Chem. Phys. 98 (1993) 1372–1377.
[43] A. Schafer, C. Huber, R. Ahlrichs, J. Chem. Phys. 100 (1994) 5829–5835.